Spectrochimica Acta Part A 71 (2008) 1525–1534

Contents lists available at ScienceDirect

Spectrochimica Acta Part A: Molecular and Biomolecular Spectroscopy

journal homepage: www.elsevier.com/locate/saa

An FTIR investigation of hexadecyltrimethylammonium intercalation into rectorite

Zhaohui Li[a,b,*], Wei-Teh Jiang[b], Hanlie Hong[c]

[a] Geosciences Department, University of Wisconsin – Parkside, Kenosha, WI 53141-2000, USA
[b] Department of Earth Sciences, National Cheng Kung University, 1 University Road, Tainan 70101, Taiwan
[c] Faculty of Earth Sciences, China University of Geosciences, Wuhan, Hubei 430074, China

ARTICLE INFO

Article history:
Received 27 March 2008
Received in revised form 4 May 2008
Accepted 12 May 2008

Keywords:
Adsorption
FTIR
HDTMA
Intercalation
Organoclay
Surfactant

ABSTRACT

Rectorite is an interstratified clay mineral made at 1:1 ratio of an orderly arrangement of a nonswelling component illite and a swelling component smectite. Due to the presence of two distinct types of components, it is of great interest to study the adsorption of long chain alkylammonium in rectorite. In this study, we conducted batch experiments and used X-ray diffraction (XRD) and Fourier Transform infrared (FTIR) spectroscopy to characterize the interlayer configuration of intercalated long chain hexadecyltrimethylammonium (HDTMA) in rectorite. The FTIR results showed that a monomer-like intercalation with extensive *gauche* conformers was formed at surfactant loading less than the cation exchange capacity (CEC) of the mineral. At a higher surfactant loading the CH_2— symmetric and anti-symmetric vibrations shifted to lower frequencies, suggesting a more ordered all-*trans* surfactant interlayer configuration. The thermogravimetric and derivative of thermogravimetric analayses showed a high pyrolysis temperature for the monomer-like *gauche* conformers and lower pyrolysis temperature for the all-*trans* configuration of the intercalated HDTMA. The XRD analysis confirmed the monomer-like conformation with a *d*-spacing of 25.2 Å at the low surfactant intercalation and a vertical all-*trans* configuration with a *d*-spacing of 49.5 Å at an HDTMA intercalation of 3.20 CEC. In addition to conformation analyses of intercalated surfactant in the interlayer using FTIR, the absorbance measured by peak height at 1470, 2850, and 2917 cm^{-1} increased linearly with surfactant loading, providing a faster, yet efficient method to quantify the amount of surfactant adsorbed.

1. Introduction

In early studies, rectorite was described as a mineral made of an alternation of one pyrophyllite unit with one vermiculite unit [1]. However, significant differences between allevardite and vermiculite were found with the former more resemble to montmorillonite as the loss of (OH) groups was found at around 900 °C without disruption of the layer structure and the organic complexes [2]. Later, it was confirmed that rectorite and allevardite were the same mineral made of mica-like (high charge, non-swelling) and montmorillonite-like (low charge, swelling) layers [3]. In a recommendation for nomenclature of regular interstratified clay minerals, rectorite was referred as an interstratified clay mineral made of regular 1:1 stacking of dioctahedral mica-like and smectite-like layers [4] that contain interlayer cations of various elements such as Na, K, and Ca [3]. The dominant interlayer cation of the mica component is used to subdivide the rectorite group into Na-, K-, or Ca-rectorite.

Due to the presence of montmorillonite component, the adsorption behavior of rectorite toward cationic surfactants would be similar to that of montmorillonite. Recent studies of using organoclays to adsorb and remove hydrophobic organic contaminants and anionic species from water showed great promises [5–8]. Similarly, uses of surfactant-modified rectorite to remove phenol and chromate have been studied recently [9,10]. However, due to the presence of two distinct types of components, it is of great interest to study the adsorption sites of long chain alkylammonium in rectorite and the interlayer configuration of intercalated/adsorbed surfactant molecules so that future modification of rectorite could be tailored toward particular needs for environmental application.

Studies on mechanisms of surfactant adsorption and intercalation into smectite minerals were conducted in great depth [11–17]. Investigation of dehydration behavior of hexadecyltrimethy-

* Corresponding author at: Geosciences Department, University of Wisconsin – Parkside, Kenosha, WI 53141-2000, USA. Tel.: +1 262 595 2487; fax: +1 262 595 2056.
E-mail address: li@uwp.edu (Z. Li).

1386-1425/$ – see front matter © 2008 Elsevier B.V. All rights reserved.
doi:10.1016/j.saa.2008.05.015

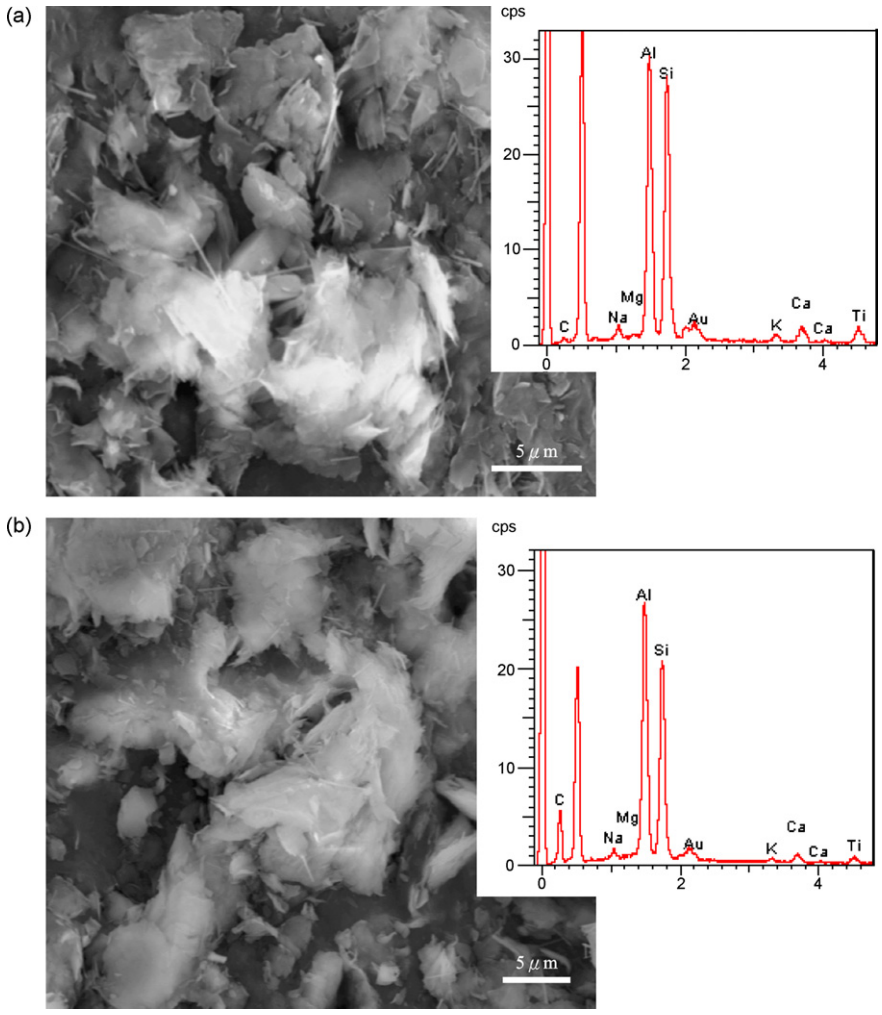

Fig. 1. SEM photographs of raw rectorite (a) and rectorite intercalated with 3.20 CEC of HDTMA (b). Inserts are EDS showing the presence of carbon after HDTMA intercalation.

lammonium (HDTMA)-exchanged smectite revealed a possible transformation from *gauche* to all-*trans* configuration of adsorbed surfactant chains during a dehydration process [13]. Fourier Transform infrared (FTIR) spectroscopy has been widely used to deduce the surface and interlayer configuration of adsorbed surfactant [11,15,17–19]. The sorbed HDTMA formed micellar-like HDTMA bromide clusters on silica surfaces at surfactant surface coverage as low as 12% at wet state, but changed from the aggregated state to a flat, parallel orientation on the silica surfaces at the dry state [18]. The adsorbed HDTMA monomers had stronger interaction with kaolinite than admicelles as the anti-symmetric vibration of CH_2 in the surfactant tail group shifted to higher frequencies at monolayer surfactant surface coverage [19]. Band shift after HDTMA intercalation into montmorillonite could be used to indicate the water content and bonding strength of adsorbed water, too. The sorbed water content decreases with the increase of intercalation of HDTMA and H_2O is less strongly hydrogen bonded as revealed by a large shift in position of the $\nu 2$ mode to higher frequencies and a small shift to lower frequencies of the stretching vibration [15].

Although extensive studies on surfactant intercalation into smectite clays have been conducted, there has been no detailed report on intercalation of alkylammonium in rectorite. Knowing the states of presence of the surfactants in the interlayer and their interlayer configuration will help us to modify the mineral more effectively toward sorption of different types of contaminants. Furthermore, conflicting results about the interlayer thickness were reported for the same clay minerals [13,16]. For these reasons, we focus our research at elucidating the surfactant interlayer configuration as a function of surfactant loading using FTIR in conjunction of X-ray diffraction (XRD) and thermogravimetric (TG) studies.

2. Experimental

2.1. Materials

The rectorite was obtained from Zhongxiang, Hubei, China. Clay fraction was separated by sedimentation followed by centrifugation. The purity of the sample was examined by scanning electron microscope (SEM) observation (Fig. 1) and XRD analyses (Fig. 2). The structural formula of the rectorite is: $(Na_{0.45}K_{0.32}Ca_{0.37}Mg_{0.08})(Al_{3.78}Fe_{0.11}Ti_{0.10})[(Si_{6.22}Al_{1.78})O_{20}](OH)_4 \cdot nH_2O$. The cation exchange capacity (CEC) is 410 $mmol_c/kg$, with Ca^{2+} and Na^+ as major exchangeable cations, indicating that the interlayer cation of the mica component is Na^+, and that of the smectite component is Ca^{2+} [9]. The specific surface area (SSA) measured by BET methods varied from 11.9 m^2/g [20] to 17 m^2/g [21].

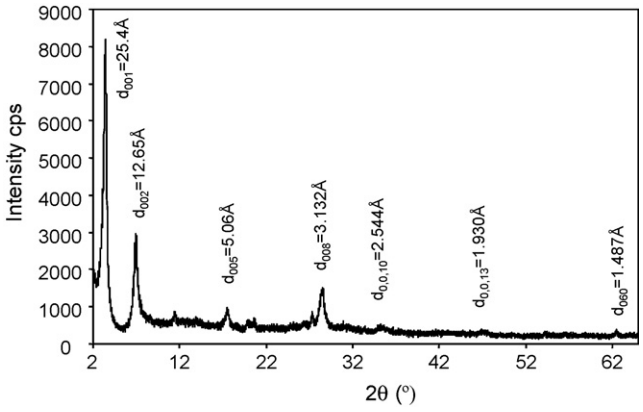

Fig. 2. XRD pattern of randomly oriented rectorite sample showing the purity of the sample. The d_{060} value indicates that the rectorite is dioctahedral.

2.2. Batch sorption experiments

The HDTMA intercalation into rectorite was performed in batch sorption experiments. For lower surfactant loading levels, 1.00 g of rectorite and 20 mL of HDTMA solution at initial concentrations of 5, 15, 25, 35, and 45 mmol/L were combined in 50 mL centrifuge tubes. While for higher surfactant loading levels, 0.50 g of rectorite and 20 mL of HDTMA solution at initial concentrations of 30, 40, and 50 mmol/L were combined. The initial inputs correspond to 0.25, 0.75, 1.25, 1.75, 2.25, 3.00, 4.00, and 5.00 CEC of the mineral. The mixture were shaken at 150 rpm for 24 h, centrifuged and the supernatant then filtered before being analyzed for equilibrium HDTMA and counterion bromide solution concentrations. The experiment was performed in duplicate.

2.3. Methods of analyses

HDTMA solution concentrations were analyzed by an HPLC method using a Shimadzu 9-A autoinjector, a Supelco C-18 column, and a Linear 100 UV–vis detector at a wavelength of 254 nm. The mobile phase was 5 mM *p*-toluenesulfonate in 45% water and 55% methanol. The retention time was 3.2 min at a flow rate of 1 mL/min. A dilution at 1/10 ratio was made for concentrations greater than 2 mmol/L. Bromide analysis was performed by another HPLC system using a Shimadzu 9-A autoinjector, a Hamilton PRP-X100 anion chromatographic column, and an Alltech electric conductivity detector. The mobile phase was 2 mM potassium phthalate with pH 6 adjusted by NaOH. The retention time was 3.1 min at a flow rate of 2 mL/min. A dilution at 1/10 ratio was made for concentrations greater than 10 mmol/L. The amount of HDTMA and bromide adsorbed was determined by the difference between the initial and equilibrium concentrations.

FTIR spectra were acquired on a PerkinElmer Spectra One Spectrometer equipped with an Attenuated Total Reflection (ATR) accessory. The spectra were obtained by accumulating 256 scans at a resolution 4 cm^{-1}.

Powder XRD analysis was performed on a Rigaku D/Max-IIIa diffractometer with Ni-filtered Cu Kα radiation at 35 kV and 20 mA. Randomly oriented samples were collected from 2° to 65° 2θ, while orientated ones from 2° to 15° 2θ. The scanning rate was 2°/min with 0.01° per step. A 1° divergent slit, 1° scatter slit and 0.3 mm receiving slit were used.

The TG analysis was performed on a Thermal Analysis model TGA 2950. The heating rate was 20 °C/min under nitrogen condition with an initial sample weight of 11–15 mg.

Table 1
Amounts of HDTMA intercalated and counterion bromide adsorbed at different initial HDTMA input

Initial HDTMA input (equivalent to CEC)	HDTMA intercalated (equivalent to CEC)	Bromide adsorbed (equivalent to CEC)	Ratio of bromide to HDTMA sorbed
0	0	0	0
0.25	0.25	0.05	0.20
0.75	0.75	0.17	0.23
1.25	1.25	0.63	0.50
1.75	1.75	0.99	0.57
2.25	2.05	1.16	0.57
3.00	2.54	1.36	0.54
4.00	2.90	1.60	0.55
5.00	3.20	1.72	0.54

3. Results and discussion

3.1. Uptake of HDTMA by rectorite

Since the CEC of the mineral is 410 $mmol_c$/kg and the initial surfactant input varied from 0.25 to 5.00 times the CEC, it is necessary to determine how much HDTMA and counterion bromide are actually adsorbed or intercalated. For this reason, the equilibrium concentrations of HDTMA and counterion bromide were measured and their adsorption/intercalation was calculated. The results showed that when initial HDTMA input was less than 2.00 CEC, the input HDTMA was completely removed from water and adsorbed or intercalated into rectorite (Table 1). As the initial input was greater than 2.00 CEC, significant amount of HDTMA is left in solution. At an initial HDTMA input of 5.00 CEC, the actual amount of HDTMA intercalated was only 3.20 CEC (Table 1), resulting in an equilibrium HDTMA solution concentration of 18 mmol/L. Accompanying HDTMA intercalation, counterion bromide was also adsorbed/intercalated into rectorite at a ratio of Br/HDTMA sorbed much less than 0.5 when input surfactant was less than the CEC and slight above 0.5 when input surfactant was greater than the CEC (Table 1). The results indicate that HDTMA adsorption/intercalation was mainly in monomer form at a low initial surfactant input and in admicellar form at a higher initial surfactant input. Energy dispersion spectrum attached to SEM showed significant increase in carbon counts (Fig. 1). In addition, the Ca counts decreased considerably compared to raw rectorite, indicating that the interlayer cation in the smectite component is made of Ca^{2+}, in an agreement with CEC measurement [9]. Randomly oriented XRD gave a d_{060} of 1.487 Å, confirming that the rectorite is dioctahedral (Fig. 2).

3.2. FTIR spectra of rectorite

The full FTIR spectra (in the range of 450–4000 cm^{-1}) of raw rectorite and rectorite intercalated with different amounts of HDTMA are plotted in Fig. 3 and the band assignment for rectorite is listed in Table 2, while that for adsorbed/intercalated HDTMA is listed in Table 3.

For the mineral rectorite, major bands of the phyllosilicate backbone are in the range of 470–1120 cm^{-1}. These bands are associated with Si—O—Si and Si—O—Al bending and stretching. As these vibrations are within the crystal structure, the adsorbed/intercalated HDTMA did not affect the linkage of Si—O and Al—O bonds. Thus, the band position remained the same even at the highest surfactant loading level (Fig. 3).

3.3. Influence of intercalated HDTMA on vibrations of water

The sharp strong vibration band at 3638 cm^{-1} is due to OH stretching vibrations of the structural OH groups, agreeing well

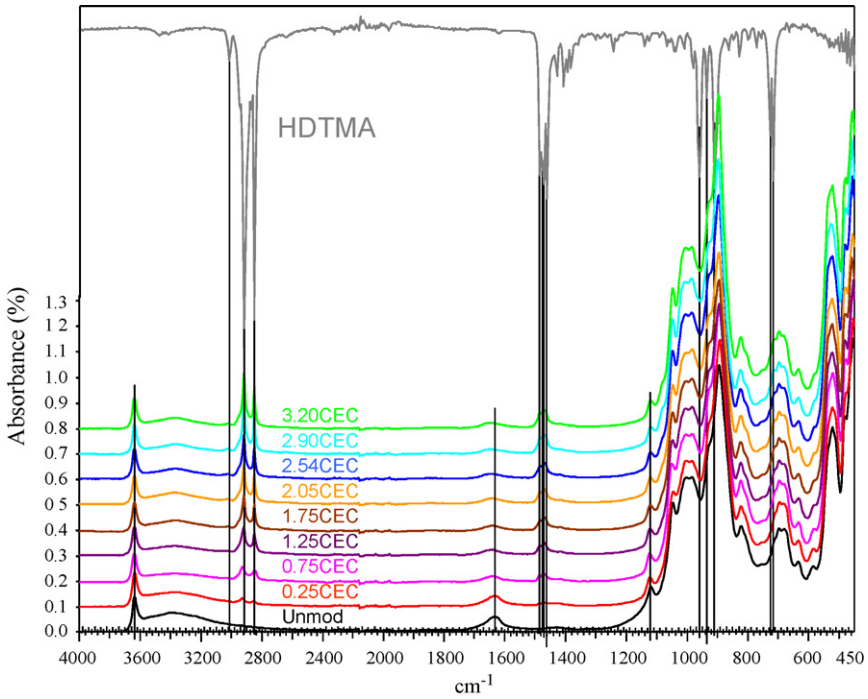

Fig. 3. FTIR spectra of rectorite intercalated with different amounts of HDTMA.

Table 2
Band positions and suggested assignments for the infrared absorption frequency of rectorite

Suggested assignment	Band positions (cm^{-1})			
	[22]	Raw rectorite this study	0.25 CEC	3.20 CEC
Si—O bending	478	479	479	480
Si—O—Al bending	545	523	523	523
Si—O—Al deformation	615	635	635	635
Si—O—Al bending	693	699	697	699
Al—O—Si in-plane	732			
Al—O—H libration	804			
Al—O out-of-plane	822	823	823	824
Al—O—H libration	875			
Al—O—H libration	914	895	895	895
In-plane Si—O—Si stretching	1021	1004	1006	1007
In-plane Si—O—Si stretching	1053	1048	1047	1048
⊥Si—O stretching	1082			
⊥Si—O stretching	1123	1120	1123	1121
H_2O bending	1639	1634	1635	1650
H_2O stretching or H-bonding to Si—O—Al linkage	3433	3390	3384	3367
Hydrogen bonding to Si—O—Si linkage	3638	3639	3638	3640

Table 3
Band assignment of alkylammonium surfactant

Assignment	Band positions (cm^{-1}) [27]	HDTMA this study
Methylene tails		
ν_{as}, CH_3—R	2956	2944
ν_{as}, CH_2	2920	2916
ν_s, CH_3—R	2870	2872
ν_s, CH_2	2850	2849
δ, CH_2 (triclinic subcell)	1472 (singlet)	
δ, CH_2 (orthorhombic subcell)	1472 + 1462 (doublet)	1473 + 1462
δ, CH_2 (hexagonal or rotator phase)	1468 (singlet)	
δ, CH_2 ("liquid-like" disorder)	1468–1466	
δ_{as}, CH_3—R	1465–1456	1431
δ, α-CH_2	1420	1397
δ_s, CH_3—R	1380	1383
Surfactant head groups		
ν_{as}, CH_3 of —$N(CH_3)_3$	3040	3032
ν_s, CH_3 of —$N(CH_3)_3$	2985	3018
δ_{as}, CH_3 of —$N(CH_3)_3$	1490, 1480	1487, 1480
δ_s, CH_3 of —$N(CH_3)_3$	1405	1408

ν = stretching, δ = bending.

with 3638 cm^{-1} for standard reference rectorite Rar-1 [22]. The location and intensity of this band are less sensitive to the HDTMA loading on rectorite (Fig. 3). For raw rectorite and rectorite intercalated with 0.25 CEC of HDTMA, the location is 3638 cm^{-1} and the intensity is 0.14% and 0.13%. The band position increased to 3640 cm^{-1} while the intensity decreased to 0.11% at HDTMA loading greater than 0.75 CEC (Table 4). Similar results were found for HDTMA modified montmorillonite [15,17].

The intercalation of surfactant had a profound effect on the adsorbed water in the interlayer. The broad band at 3200–3560 cm^{-1} was originated from absorbed water and thus is strongly affected by the surfactant loading. For raw rectorite and rectorite intercalated to 0.25 CEC, the peak is located at 3390, and 3384 cm^{-1} (Fig. 3). However, as the intercalated increased to 0.75 CEC, the location of the absorption band shifted to 3367 cm^{-1}. Meanwhile, the absorbance intensity of the broad band was 0.08% for raw rectorite. It decreased to 0.07% at 0.25 CEC loading, and further decreased to 0.04% when intercalated HDTMA was 0.75 CEC and remained the same even though the HDTMA loading increased further (Table 4). Similar effects were found for HDTMA modified montmorillonite [15,17]. The decrease in vibration frequency was attributed to the decrease in hydrogen bonding strength in organomontmorillonites [15], as H_2O content is reduced with an increase in surfactant intercalation into the interlayer.

The absorption band related to the $\nu 2$(H—O—H) bending vibration of water molecules sorbed on rectorite was also strongly affected by the amount of HDTMA adsorbed/intercalated (Fig. 4). The band centered at 1634 cm^{-1} with a peak absorbance of 0.053 for raw rectorite. The frequency remained at 1634 cm^{-1} while the peak absorbance decreased to 0.037 at an HDTMA loading of 0.25 CEC (Table 4). As the HDTMA loading increased to 0.75 CEC, the band center shifted to 1641 cm^{-1} while the peak absorbance further decreased to 0.023. At an HDTMA loading of 1.75 CEC, the frequency increased to 1650 cm^{-1} while the peak absorbance decreased to 0.018 and remained the same with further increases in HDTMA loading. The decrease in intensity reflects that the amount of water in the interlayer is reduced as the amount of intercalated HDTMA increased and is confirmed by TG analysis (see later). The shift to a higher frequency indicated that the residual water molecules are held tighter due to stronger interaction, also confirmed by TG analysis. Similar results were observed for HDTMA adsorption on Al-montmorillonite [17]. The trend of band shifting toward a higher frequency with an increase in HDTMA intercalation was attributed to increased hydrophobicity of the resultant materials [17]. However, such interpretation may not be logic since at a surfactant loading level greater than 2.0 CEC, the surface becomes more hydrophilic compared to lower surfactant loading levels due to the reversal of surface charge and exposed ammonium groups on outermost surface as revealed by electrophoretic mobility measurement [23] and turbidity measurement [24].

3.4. Influence of intercalated HDTMA on vibration frequencies

The vibration bands of the surfactant can be groups into two categories: those associated with methylene tails and those with alkylammonium head groups. The peak around 3018 cm^{-1} was assigned to the symmetric stretching mode ν_s of the trimethylammonium headgroup CH_3—N of HDTMA [25,26] while the peak at 3040 cm^{-1} was assigned to the anti-symmetric stretching mode ν_{as} of CH_3—N of HDTMA [27]. In this study these two peaks are well resolved at 3018 and 3032 cm^{-1} for HDTMA solid (Fig. 5). For rectorite intercalated with 2.05 CEC of HDTMA and above, the ν_s of CH_3—N is clearly visible, indicating that the intercalated HDTMA resembles more to HDTMA solid (Figs. 3 and 5). Furthermore, for HDTMA solid, the ν_{as} and ν_s of CH_3—R are located at 2944 and 2872 cm^{-1} (Fig. 5). The ν_s CH_3—R is clearly visible at an HDTMA intercalation of 2.05 CEC and above, again indicating that the intercalated HDTMA resembles more to HDTMA solid (Fig. 5). However, these bands were not reported in previous studies [15,17].

The CH_2 stretching bands near 2917 and 2850 cm^{-1} are generally the strongest bands. The frequency, width, peak height, and integrated intensity of these ν_{as} and ν_s bands are sensitive to the *gauche*/*trans* conformer ratio of the hydrocarbon chains. A shift from low frequencies characteristic of highly ordered, all-*trans* conformations, to higher frequencies and increased width is accompanied as the number of *gauche* conformers (the "disorder" of the chain) increases [27]. At an HDTMA intercalation of 0.25 CEC, these bands were located at 2930 and 2856 cm^{-1}, reflecting a large number of *gauche* conformers intercalated into or adsorbed onto rectorite (Fig. 5). At 0.75 CEC, these bands shifted to 2928 and 2850 cm^{-1}, revealing a decrease in the number of *gauche* conformers in rectorite. As the HDTMA intercalated/adsorbed further increased to 1.25 CEC, the ν_{as}, CH_2 band further shifted to 2921 cm^{-1}, while the ν_s, CH_2 band remained at 2850 cm^{-1} (Table 5). Further increases in HDTMA loading beyond 1.75 CEC resulted in minor shift of the ν_{as}, CH_2 to 2918 cm^{-1}, slightly larger than that of pure solid HDTMA of 2916 cm^{-1}, while the ν_s, CH_2 band remained at 2850 cm^{-1} contrast to 2849 cm^{-1} for pure solid HDTMA. The location of these bands revealed that an all-*trans* arrangement of intercalated HDTMA could be achieved at the HDTMA loading approximately equal to twice of the CEC of the minerals. These band positions were located at 2920 and 2851 cm^{-1} for kaolinite modified by HDTMA to a bilayer surfactant surface coverage [19], at 2917 and 2849 cm^{-1} for montmorillonite modified by HDTMA to 200% CEC [15], and at 2921 ad 2851 cm^{-1} for Al-montmorillonite modified by HDTMA to 300% CEC [17].

The FTIR absorption bands at 1450–1480 and 710–740 cm^{-1}, corresponding to the methylene scissoring mode and methylene rocking mode, are also sensitive to the interchain interactions and are diagnostic of the packing arrangements in alkyl chain assemblies [28,29]. Further more the band remains as a singlet or splits into a doublet depended on the conformation of methylene tail

Table 4
Vibration of H_2O molecules as affected by the amount HDTMA intercalated

HDTMA intercalated (equivalent to CEC)	Hydrogen bonding to Si—O—Si linkage		$\nu 1$ H_2O stretching or H-bonding to Si—O—Al linkage		$\nu 2$ H_2O bending vibration	
	Location (cm^{-1})	Abs. (%)	Location (cm^{-1})	Abs. (%)	Location (cm^{-1})	Abs. (%)
0	3638	0.14	3390	0.08	1634	0.053
0.25	3638	0.13	3384	0.07	1635	0.034
0.75	3640	0.11	3367	0.03	1641	0.023
1.25	3640	0.11	3367	0.04	1645	0.018
1.75	3640	0.11	3367	0.04	1650	0.018
2.05	3640	0.11	3367	0.04	1650	0.018
2.54	3640	0.11	3367	0.04	1650	0.018
2.90	3640	0.11	3367	0.04	1650	0.018
3.20	3640	0.11	3367	0.04	1650	0.019

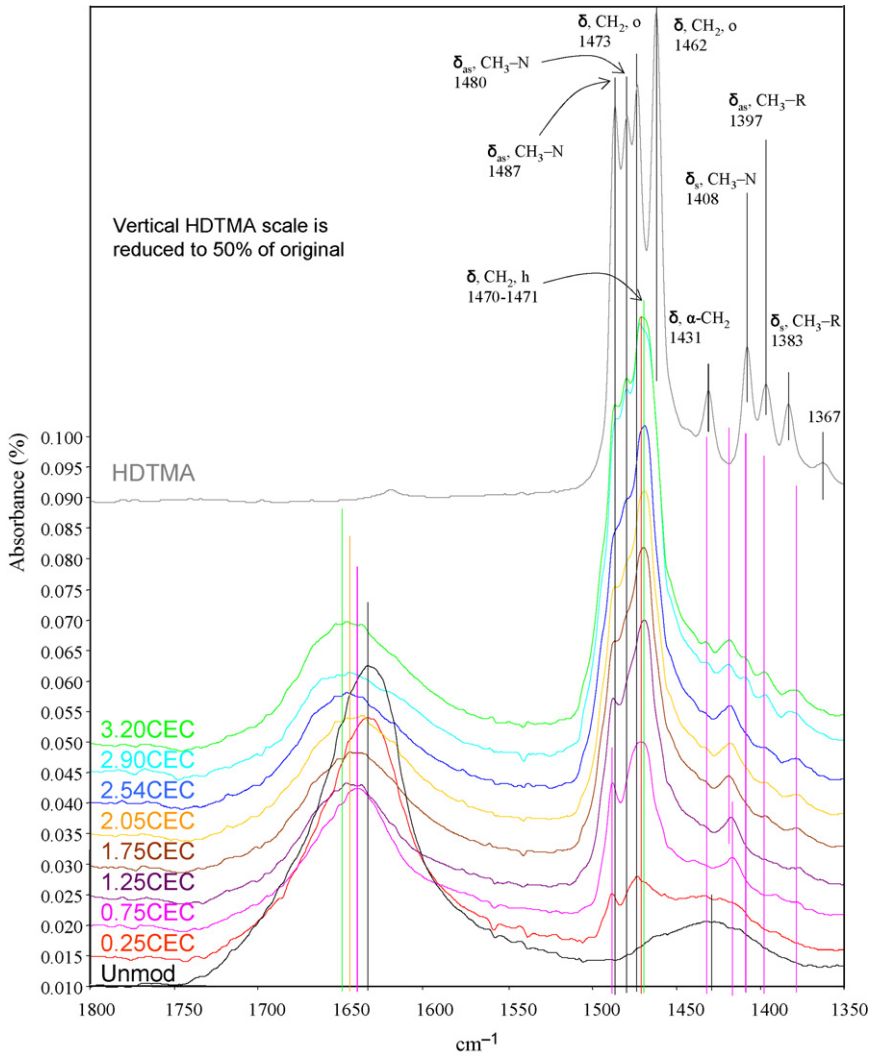

Fig. 4. FTIR spectra of the H—O—H bending region at 1634–1650 cm^{-1} and the C—H bending at 1467–1472 cm^{-1} showing the peak shift and change in intensity as a function of HDTMA intercalated.

groups. A sharp narrow singlet is found at 1472 cm^{-1} when the methylene chains are packed in an all parallel arrangement descried as triclinic subcell or at 1468 cm^{-1} for a hexagonal phase [27]. A doublet at 1462 and 1473 cm^{-1} indicates an orthorhombic subcell [27]. The split of the methylene scissoring and rocking bands is a reflection of the intermolecular interaction between the two adjacent hydrocarbon chains and the split is more pronounced at lower temperature with an orthorhombic subcell [28]. For pure HDTMA solid, a doublet is found at 1462 and 1473 cm^{-1} for the scissoring mode, and at 715 and 728 cm^{-1} for the rocking mode, indicating an orthorhombic subcell. At 0.25 CEC loading, the band is a singlet located at 1472 cm^{-1}, reflecting that the surfactant surface arrangement is similar to that of a triclinic subcell and it decreased to 1470 cm^{-1} at HDTMA loading at 1.25 CEC, suggesting a change to hexagonal phase (Fig. 4 and Table 3).

Due to the strong peak of Si–O–Al bending at 699 cm^{-1}, the 720 and 730 cm^{-1} peaks fall on the side of this strong peak. They showed up as two shoulders at an HDTMA intercalation

Table 5
Vibration of HDTMA as affected by the amount intercalated

HDTMA intercalated (equivalent to CEC)	C—H asymmetric stretching		C—H symmetric stretching		C—H bending	
	Location (cm^{-1})	Abs. (%)	Location (cm^{-1})	Abs. (%)	Location (cm^{-1})	Abs. (%)
0	–	–	–	–	–	–
0.25	2930.0	0.018	2855.6	0.010	1473.2	0.008
0.75	2928.0	0.038	2849.7	0.030	1470.4	0.024
1.25	2920.8	0.080	2850.4	0.059	1469.1	0.039
1.75	2919.2	0.110	2850.3	0.078	1469.1	0.044
2.05	2918.7	0.123	2850.5	0.088	1469.1	0.048
2.54	2918.3	0.140	2850.4	0.099	1469.1	0.053
2.90	2918.1	0.185	2850.0	0.132	1468.0	0.063
3.20	2918.0	0.182	2849.0	0.133	1467.0	0.060

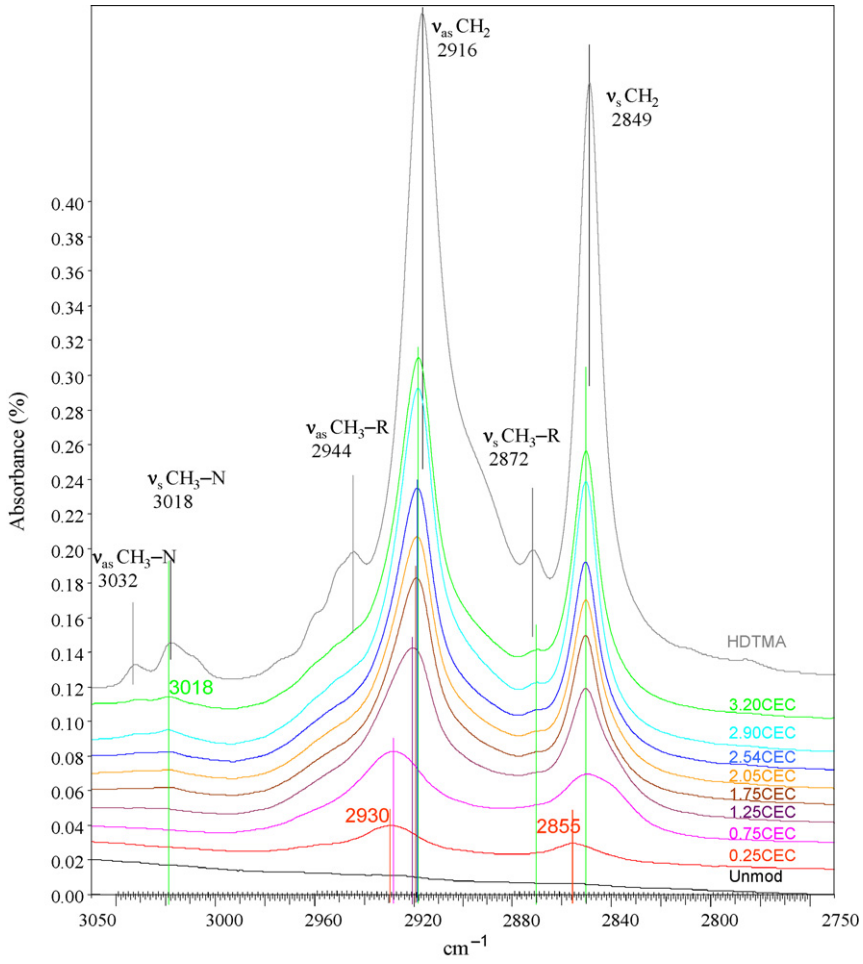

Fig. 5. FTIR spectra of the CH_2 stretching bands showing the peak shift and change in intensity as a function of HDTMA intercalated.

of 2.00 CEC or less. Above 2.00 CEC intercalation, a separate peak appeared at 712 cm^{-1} while a shoulder peak appeared at 731 cm^{-1}. The results indicate that when the amount of HDTMA intercalated was greater than 2.00 CEC, all-*trans* conformers began to appear and were further developed as the surfactant loading increased.

The band at 1484 cm^{-1} is due to the anti-symmetric bending mode of the head [$(CH3)_3N^+$—] methyl group and is sensitive to the extent of disorder and the packing of the headgroup [25,27]. For micellar systems it is made of a doublet at 1480 and 1490 cm^{-1} [27]. The doublet is located at 1480 and 1487 cm^{-1} for solid HDTMA (Fig. 4). When HDTMA loading levels were low, a single peak is located at 1488 cm^{-1} and it is gradually shifted to 1486 cm^{-1} at an HDTMA intercalation greater than 1.75 CEC. A doublet appeared at an HDTMA intercalation of 2.05 CEC and above, suggesting an admicellar configuration for intercalated/adsorbed HDTMA molecules that resembled more to that of solid HDTMA (Fig. 4). These results indicate that the headgroups of HDTMA are attached to the aluminosilicate layer surface with a relatively high order at a higher HDTMA loading.

The bands at 1383–1431 cm^{-1} are assigned to scissoring modes of δ_s, CH_3—R (1383 cm^{-1}), δ_{as}, CH_3—R (1397 cm^{-1}), δ_s, CH_3—N (1408 cm^{-1}), and δ, α-CH_2 (1431 cm^{-1}). The last one is the scissoring band of methylene groups adjacent to a positively charged nitrogen [27]. At low surfactant loading, only δ_s, CH_3—N appeared. However, its location shift to a higher frequency significantly compared to solid HDTMA. At higher surfactant loading levels, all four absorption bands appeared and all shifted to higher frequencies significantly (Fig. 4). The location these bands may reflect differences between crystalline HDTMA and HDTMA intercalated into the interlayer of clay minerals.

In addition to the location of vibration bands for methylene tails, the intensity of absorbance bands for the ν_{as}, CH_2, ν_s, CH_2, and δ, CH_2 as indicated by peak height have strong linear correlations with the amount of HDTMA intercalated/adsorbed (Fig. 6). The regression coefficients (r^2) are 0.99 for the first two and 0.94 for the last

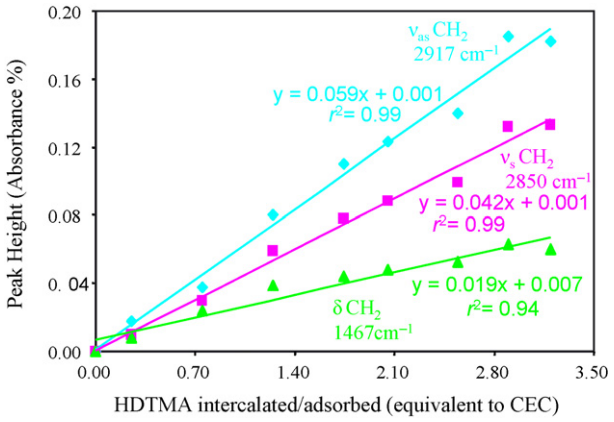

Fig. 6. Change in FTIR absorbance as affected by amounts of HDTMA intercalated.

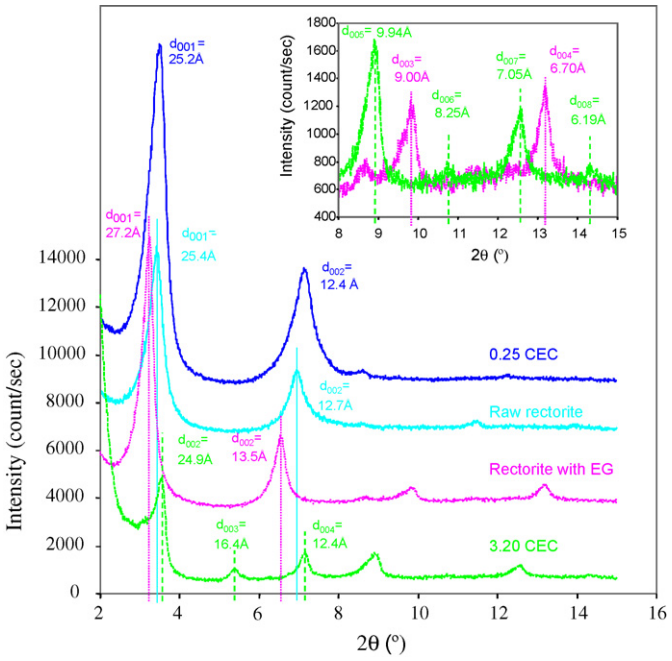

Fig. 7. XRD patterns of raw rectorite, EG-saturated, HDTMA intercalated rectorite at 0.25 and 3.20 CEC. The inserts show (0 0 5) to (0 0 8) for 3.20 CEC intercalation.

one. Thus, the absorbance intensity as expressed by peak height could be used as a convenient method to quantitatively determine the amount of HDTMA intercalated/adsorbed.

3.5. XRD analyses

To further elucidate the intercalation of HDTMA into the interlayer of rectorite, ethylene glycol (GE) saturated rectorite, and rectorite intercalated at 0.25 and 3.20 CEC of HDTMA were subjected to XRD analysis. Strong (0 0 *l*) reflections with *l* = 1, 2, 5, 8, and 13 were reported for rectorite [1,30]. All these reflections plus *l* = 10 were observed for this rectorite (Fig. 2). The d_{001} spacing of the raw rectorite is 25.4 Å, typical for a rectorite made of an illite component and a Ca-montmorillonite component. The d_{001} spacing increased to 27.2 Å, showing the expansion of smectite layer after GE solvation. At HDTMA intercaltion of 0.25 CEC, the d_{001} spacing decreased slightly from 25.4 to 25.2 Å. However, the d_{002} spacing decreased much more from 12.7 to 12.4 Å. At the maximum HDTMA intercalation of 3.20 CEC, the (0 0 1) peak of the HDTMA-intercalated rectorite is missing. However, the (0 0 2) to (0 0 8) reflections were well reflected (Fig. 7) and the *d*-spacing of HDTMA intercalated rectorite determined from these reflections is 49.5 ± 0.2 Å. For such a larger d_{001} the 2θ angle is less than 2°, the lowest angle that the XRD was recorded.

3.6. TG and DTG analyses

The TG and DTG curves of rectorite intercalated with initial HDTMA of 0.25 and 3.20 CEC together with those of solid HDTMA are presented in Fig. 8. The change in mass falls into three regions for HDTMA intercalated rectorite: less than 200, 230–280, and 420–450 °C. On the contrary, the mass loss of solid HDTMA occurred in a single temperature range. The onset temperature (T_{onset}) was 236 °C while the temperature corresponding to the highest rate of mass loss (T_{peak}) was at 262 °C for pure HDTMA (Fig. 8a). This T_{peak} is much higher than 202 °C in one report [31] and much lower than 322 °C in another report [32].

At an HDTMA intercalation of 0.25 CEC, the mass loss due to removal of adsorbed water (for $T < 200$ °C) accounted for 5% of the total mass. In contrast, after intercalated with 3.20 CEC of HDTMA, the amount of mass loss due to the removal of adsorbed water was reduced to 2% (step 1). For rectorite intercalated with 0.25 CEC of HDTMA, the next mass loss occurred after 400 °C (Fig. 8b), with the percentage of mass loss corresponding to 3.1% and T_{peak} at 440 °C. On the other hand, at HDTMA intercalation of 3.20 CEC, the second step of mass loss had a T_{onset} of 195 °C and a T_{peak} of 232 °C, while the third step of mass loss had a T_{onset} of 395 °C and a T_{peak} of 430 °C (Fig. 8b). For a montmorillonite intercalated with 2.50 CEC of HDTMA, the T_{peak} was at 205 and 380 °C for the second and third mass loss [31]. In addition, the mass loss in steps 2 and 3 accounted for 24 and 5%, respectively. The TG and DTG analysis of rectorite intercalated with 3.20 CEC of HDTMA suggested two distinct states for the intercalated surfactant molecules: the one associates with stronger interaction and thus requires a higher degree of temperature to decompose and the one with weaker interaction whose decomposition temperature was slightly lower than that of pure HDTMA solid. In the first state of presence, the intercalated HDTMA adopted a monomer-like *gauche* arrangement in the interlayer of montmorillonite component in rectorite. For the second state of presence, HDTMA formed an all-*trans* admicellar-like intercalation in rectorite. The results are in an agreement with the FTIR study of intercalated HDTMA in rectorite and with the trend in HDTMA intercalation in montmorillonite [15–17].

3.7. HDTMA interlayer configuration

The rectorite is a 1:1 regular interstratified clay mineral made of alternations of illite and montmorillonite layers. When organic molecules are intercalated into montmorillonite, the expansion of d_{001} is due to removal of interlayer water and intercalation of organic molecules. For example, when intercalated alkylammonium adopted a flat-lying orientation in montmorillonite with a

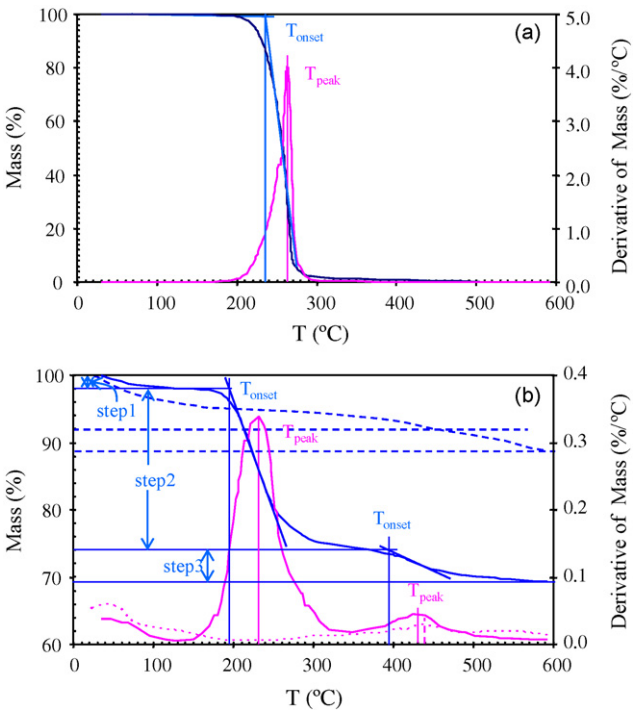

Fig. 8. TG and DTG analysis of solid HDTMA (a) and HDTMA intercalated rectorite at 0.25 CEC (dashed lines) and 3.20 CEC (solid lines).

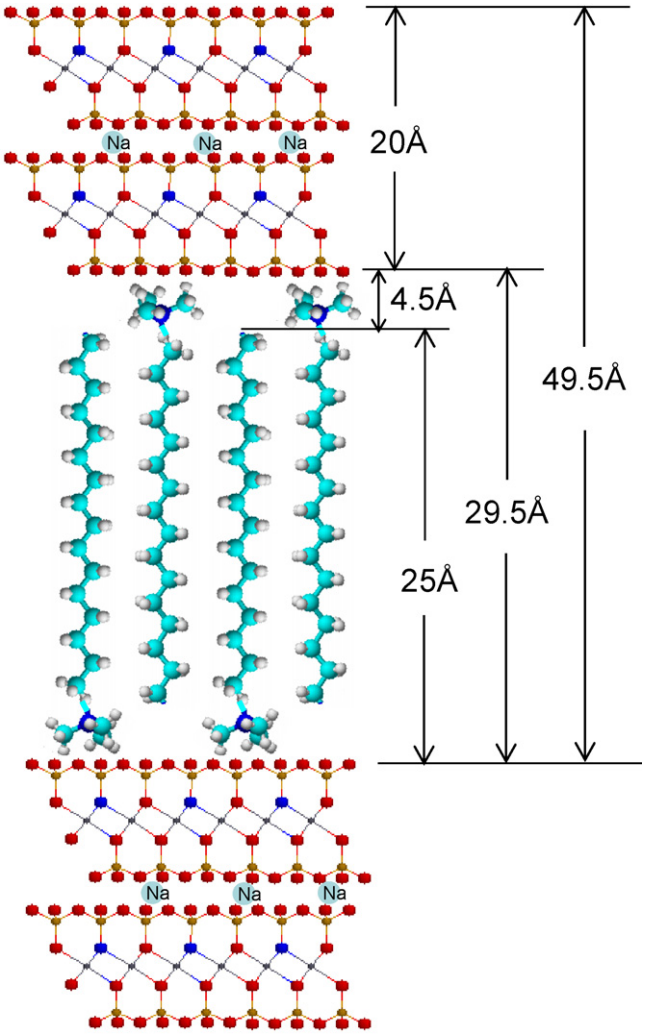

Fig. 9. Illustration of vertical arrangement of intercalated HDTMA molecules in the interlayer space of montmoriilonite component in rectorite.

surfactant chain length less than 8 carbons, the *d*-spacing changed to 13.5 Å, made of a dehydrated montmorillonite layer (same as an illite layer) of 10 Å together with the flat-lying monolayer of 3.5 Å [11,33]. At the HDTMA loading of 1.0 CEC the *d*-spacing of a Na-montmorillonite SWy and a Ca-montmorillonite SAz expanded to 24 and 18 Å, respectively [13]. For the same SWy and SAz at an initial HDTMA loading of 3.0 CEC, the *d*-spacing expanded to 20 and 40 Å, respectively [16]. Separately, the *d*-spacing of an Al-montmorillonite expanded to 38 Å after modified by HDTMA at an initial loading of 3.0 CEC [17]. Compared to these results, it is not surprised to see the gallery height of 49.5 Å for rectorite at 3.20 CEC intercalation. The chain length of the HDTMA is about 25 Å [16], in which 21 Å is for the tail group and 4 Å is for the head group. For a vertical surfactant bilayer intercalation in rectorite, the tail group plus two head groups will be about 29 Å and the overall *d*-spacing will be 49 Å (Fig. 9). This new *d*-spacing confirms that the intercalation of HDTMA was only to the interlayer of montmorillonite component and the interlayer of illite remained un-intercalated. It was demonstrated that the adsorbed HDTMA on zeolite adopted a densely packed HDTMA configuration due to strong hydrophobic tail–tail interactions [23]. As a matter of fact, the 40 Å *d*-spacing when HDTMA was intercalated into Ca-montmorillonite at a higher initial surfactant loading as studied by Lee et al. [16] might as well be originated from the same surfactant interlayer configuration. A strong tail–tail interaction as depicted in Fig. 9 should be thermodynamically favored with the confirmation of d_{001} spacing from XRD, the lower pyrolysis temperature from TG and DTG, and the all-*trans* conformation from FTIR.

4. Conclusions

The interlayer configuration of intercalated HDTMA in rectorite was affected by the amount of surfactant intercalated as revealed by FTIR and supported by XRD, TG, and DTG analyses. When the amount of surfactant intercalated is less than the CEC of the minerals, the surfactant molecules adopt a monomer-like *gauche* arrangement in the inter layer as revealed by the shift of symmetric and anti-symmetric stretching vibrations of the methylene tail group. As the surfactant intercalated is approaching to 2.00 CEC, a more ordered all-*trans* interlayer configuration was achieved as revealed by the shift of CH_2— symmetric and anti-symmetric vibration to the lower frequencies and by the appearance of a doublet for the anti-symmetric bending mode of the [$(CH3)_3N^+$—] headgroup at 1484 cm^{-1}. Meanwhile, at this intercalation level, the ratio of counterion intercalated to surfactant intercalated is about 1:2, indicating a bilayer surfactant interlayer configuration with half of positive charges of the HDTMA headgroup balanced by the counterion. The *d*-spacing of 25.2 Å at 0.25 CEC intercaltion confirmed the monomer-like arrangement of the intercalated HDTMA molecules with a horizontal orientation. In contrast, the *d*-spacing of 49.5 Å after intercalated with 3.2 CEC of HDTMA indicated a vertical arrangement of the intercalated HDTMA molecules in the interlayer, resulting in a full extended gallery height equal to the sum of an illite layer, a dehydrated montmorillonite layer (same as an illite thickness), HDTMA tail group plus two headgroups in opposite direction. The TG and DTG analyses indicated a higher pyrolysis temperature for the monomer-like *gauche* conformers and a lower pyrolysis temperature for micellar-like all-*trans* conformers, agreeing well with the observations of FTIR. In addition to structural information revealed by FTIR, the peak heights of the absorbance of the three methylene vibrations, symmetric and anti-symmetric stretching vibrations and the CH_2 bending vibration, are linearly proportional to the amount of HDTMA intercalated and could be used as a fast and convenient method to quantify the amount of surfactant loading on clays.

Acknowledgments

Funding from National Cheng Kung University (NCKU) for the project of Promoting Academic Excellence & Developing World Class Research Centers to support Li's sabbatical stay in NCKU is greatly appreciated.

References

[1] W.F. Bradley, Am. Miner. 35 (1950) 590.
[2] G.W. Brindley, Am. Miner. 41 (1956) 91.
[3] G. Brown, A.H. Weir, in: I.Th. Rosenquist, P. Graff-Petersen (Eds.), Proceedings of International Clay Conference, 1963, vol. 1, Stockholm, 1963, p. 27.
[4] S.W. Bailey, G.W. Brindley, H. Kodama, R.T. Martin, Clays Clay Miner. 30 (1982) 76.
[5] M.M. Mortland, S. Shaobai, S.A. Boyd, Clays Clay Miner. 34 (1986) 581.
[6] L.J. Michot, T.J. Pinnavaia, Clays Clay Miner. 39 (1991) 634.
[7] Z. Li, J. Environ. Qual. 29 (1999) 1457.
[8] B.S. Krishna, D.S.R. Murty, B.S. Jai Prakash, Appl. Clay Sci. 20 (2001) 65.
[9] H.L. Hong, W.-T. Jiang, X. Zhang, L. Tie, Z. Li, Appl. Clay Sci., in press.
[10] Y. Huang, X. Ma, G. Liang, H. Yan, Chem. Eng. J., in press.
[11] R.A. Vaia, R.K. Teukolsky, E.P. Giannelis, Chem. Mater. 6 (1994) 1017.
[12] S. Xu, S.A. Boyd, Langmuir 11 (1995) 2508.
[13] S.Y. Lee, S.J. Kim, Geosci. J. 7 (2003) 203.
[14] Y. Xi, Z. Ding, H. He, R.L. Frost, J. Colloid Interface Sci. 277 (2004) 116.
[15] H.P. He, R.L. Frost, J. Zhu, Spectrochim. Acta A 60 (2004) 2853.

[16] S.Y. Lee, W.J. Cho, P.S. Hahn, M. Lee, Y.B. Lee, K.J. Kim, Appl. Clay Sci. 30 (2005) 174.
[17] H. Xue, H. He, J. Zhu, P. Yuan, Spectrochim. Acta A 67 (2007) 1030.
[18] K. Kung, K.F. Hayes, Langmuir 9 (1993) 263.
[19] Z. Li, L. Gallus, Colloid Surf. A 264 (2005) 61.
[20] P. Chang, S. Yu, T. Chen, A. Ren, C. Chen, X. Wang, J. Radioanal. Nucl. Chem. 274 (2007) 153.
[21] G. Zhang, X. Yang, Y. Liu, Y. Jia, G. Yu, S. Ouyang, J. Colloid Interface Sci. 278 (2004) 265.
[22] J.T. Kloprogge, R.L. Frost, L. Hickey, J. Mater. Sci. Lett. 18 (1999) 1921.
[23] Z. Li, R.S. Bowman, Environ. Sci. Technol. 32 (1998) 2278.
[24] G.R. Rakhshandehroo, R.B. Wallace, X. Zhao, S.A. Boyd, T.C. Voice, J. Environ. Eng. 127 (2001) 724.
[25] T.C. Wong, N.B. Wong, P.A. Tanner, J. Colloid Interface Sci. 186 (1997) 325.
[26] R.A. Campbell, S.R. Parker, J.P.R. Day, C.D. Bain, Langmuir 20 (2004) 8740.
[27] J.G. Weers, D.R. Scheuing, in: D.R. Scheuing (Ed.), Fourier Transform Infrared Spectroscopy in Colloidal and Interface Science, ACS Symposium Series 447, American Chemical Society, Washington, DC, 1990, p. 87.
[28] H.L. Casal, H.H. Mantsch, D.G. Cameron, R.G. Snyder, J. Chem. Phys. 77 (1982) 2825.
[29] N.V. Venkataraman, S. Vasudevan, J. Phys. Chem. B 105 (2001) 1805.
[30] S. Shimoda, T. Sudo, Am. Miner. 45 (1960) 1069.
[31] Q. Zhou, R.L. Frost, H. He, Y. Xi, J. Colloid Interface Sci. 307 (2007) 50.
[32] A. Vazquez, M. López, G. Kortaberria, L. Martín, I. Mondragon, Appl. Clay Sci., in press.
[33] G. Lagaly, M.F. Gonzalez, A. Weiss, Clay Miner. 11 (1976) 173.